Effect of Surfactant on Interfacial Gas Transfer Studied by Axisymmetric Drop Shape Analysis−Captive Bubble (ADSA-CB)

Yi Y. Zuo,[†] Dongqing Li,[†] Edgar Acosta,[‡] Peter N. Cox,[§] and A. Wilhelm Neumann*,[†]

Department of Mechanical and Industrial Engineering, University of Toronto, 5 King's College Road, Toronto, ON, M5S 3G8, Canada, Department of Chemical Engineering and Applied Chemistry, University of Toronto, 200 College Street, Toronto, ON, M5S 3E5, Canada, and Department of Critical Care Medicine, The Hospital for Sick Children, 555 University Avenue, Toronto, ON, M5G 1X8, Canada

Received January 31, 2005. In Final Form: April 3, 2005

A new method combining axisymmetric drop shape analysis (ADSA) and a captive bubble (CB) is proposed to study the effect of surfactant on interfacial gas transfer. In this method, gas transfer from a static CB to the surrounding quiescent liquid is continuously recorded for a short period (i.e., 5 min). By photographical analysis, ADSA-CB is capable of yielding detailed information pertinent to the surface tension and geometry of the CB, e.g., bubble area, volume, curvature at the apex, and the contact radius and height of the bubble. A steady-state mass transfer model is established to evaluate the mass transfer coefficient on the basis of the output of ADSA-CB. In this way, we are able to develop a working prototype capable of simultaneously measuring dynamic surface tension and interfacial gas transfer. Other advantages of this method are that it allows for the study of very low surface tensions (<5 mJ/m^2) and does not require equilibrium of gas transfer. Consequently, reproducible experimental results can be obtained in a relatively short time. As a demonstration, this method was used to study the effect of lung surfactant on oxygen transfer. It was found that the adsorbed lung surfactant film shows a retardation effect on oxygen transfer, similar to the behavior of a pure DPPC film. However, this retardation effect at low surface tensions is less than that of a pure DPPC film.

1. Introduction

The effect of surfactants on the interfacial mass transfer between two phases (e.g., gas−liquid, liquid−liquid, solid−liquid) has been extensively studied due to its crucial importance in a variety of industrial, environmental, and biological fields, such as liquid−liquid extraction,[1] design and optimization of two-phase reactors,[2] metal corrosion prevention,[3] water conservation,[4] wastewater treatment,[5] water pollution monitoring,[6,7] industrial fermentations,[8] and culture of microorganisms.[9]

Both theoretical[10−18] and experimental[19−26] studies were conducted using a variety of models. These models can be divided into two categories: the moving drop/bubble model and the stagnant-film model. By means of these models, previous studies have suggested that the effects of surfactant on interfacial mass transfer are largely attributed to two mechanisms: the hydrodynamic effects and the physicochemical effects.

The hydrodynamic effects are usually studied by the so-called moving drop/bubble models, in which the effect of surfactant on interfacial mass transfer is examined by monitoring the movement and dissolution of a single falling drop or rising bubble in an aqueous continuum.[19−23] The hydrodynamic effects on a moving drop/bubble due to the addition of surfactant are to retard the internal circulation and to reduce the velocity of fall or rise. For a moving drop/bubble, surfactants tend to condense in the rear of the drop/bubble to form a "stagnant surfactant cap", which renders that part of interface rigid and causes

* Author to whom correspondence should be addressed. Tel: +1−416-978-1270. Fax: +1−416-978-7753. E-mail: neumann@mie.utoronto.ca.

[†] Department of Mechanical and Industrial Engineering, University of Toronto.

[‡] Department of Chemical Engineering and Applied Chemistry, University of Toronto.

[§] The Hospital for Sick Children.

(1) Thorsen, G.; Terjesen, S. G. *Chem. Eng. Sci.* **1962**, *17*, 137.
(2) Schaftlein, R. W.; Russell, T. W. F. *Ind. Eng. Chem.* **1968**, *60*, 12.
(3) Yapar, S.; Peker, S. *Colloids Surf., A* **1999**, *149*, 307.
(4) Barnes, G. T. *Colloids Surf., A* **1997**, *126*, 149.
(5) Wagner, M.; Pöpel, H. J. *Water Sci. Technol.* **1996**, *34*, 249.
(6) Masutani, G. K.; Stenstrom, M. K. *J. Environ. Eng.* **1991**, *117*, 126.
(7) Mölder, E.; Tenno, T.; Nigu, P. *Crit. Rev. Anal. Chem.* **1998**, *28*, 75.
(8) Tsao, G. T.; Lee, D. D. *AIChE J.* **1975**, *21*, 979.
(9) Sheppard, J. D.; Cooper, D. G. *J. Chem. Technol. Biotechnol.* **1990**, *48*, 325.
(10) Levich, V. G. *Physicochemical Hydrodynamics*; Prentice Hall: Englewood Cliffs, NJ, 1962.
(11) Lochiel, A. C. *Can. J. Chem. Eng.* **1965**, *43*, 40.
(12) Ruckenstein, E. *Chem. Eng. Sci.* **1964**, *19*, 505.
(13) Duda, J. L.; Vrentas, J. S. *Chem. Eng. Sci.* **1967**, *22*, 27.
(14) Meijboom, F. W.; Vogtländer, J. G. *Chem. Eng. Sci.* **1974**, *29*, 857.
(15) Vogtländer, J. G.; Meijboom, F. W. *Chem. Eng. Sci.* **1974**, *29*, 949.
(16) Quintana, G. C. *Int. J. Heat Mass Transfer* **1990**, *33*, 2631.
(17) Liao, Y.; McLaughlin, J. B. *J. Colloid Interface Sci.* **2000**, *224*, 297.
(18) Ponoth S. S.; McLaughlin J. B. *Chem. Eng. Sci.* **2000**, *55*, 1237.
(19) Calderbank P. H.; Lochiel, A. C. *Chem. Eng. Sci.* **1964**, *19*, 485.
(20) Vogtländer, J. G.; Meijboom, F. W. *Chem. Eng. Sci.* **1974**, *29*, 799.
(21) Koide, K.; Hayashi, T.; Sumino, K.; Iwamoto, S. *Chem. Eng. Sci.* **1976**, *31*, 963.
(22) Mekasut, L.; Molinier, J.; Angelino, H. *Chem. Eng. Sci.* **1978**, *33*, 821.
(23) Sharifullin, V. N.; Luebbert, A. *Theor. Found. Chem. Eng.* **2002**, *36*, 230.
(24) Hawke, J. G.; Parts, A. G. *J. Colloid Sci.* **1964**, *19*, 448.
(25) Plevan, R. E.; Quinn, J. A. *AIChE J.* **1966**, *12*, 894.
(26) Burnett, J. C.; Himmelblau, D. M. *AIChE J.* **1970**, *16*, 185.

10.1021/la050281u CCC: $30.25
Published on Web 05/03/2005

the Marangoni effect.[12] The Marangoni effect generated by the surface tension gradient can significantly reduce the internal circulation of a moving drop/bubble, thus attenuating the contribution of local convective mass transfer. The retardation in interfacial mass transfer due to the hydrodynamic effects is only significant for moving interfaces. By eliminating the movement of mass transfer interfaces, the effect of hydrodynamics is largely diminished.

The physicochemical effects refer to the direct blocking effects of surfactant molecules adsorbed at the interface on the transport of solute molecules by altering the physicochemical properties of the interface.[27,28] Generally, the surfactant molecules adsorbed at a two-phase interface perform as (1) a steric barrier, i.e., to decrease the available interfacial area for diffusion of the solute molecules and (2) an energy barrier, i.e., to increase the surface viscosity and the thickness of the mass transfer interface by forming a hydration layer, in which water molecules are highly oriented. The physicochemical effects due to the addition of surfactants are also commonly referred to as an "interfacial resistance" or "barrier". The interfacial resistance exists for both static and mobile interfaces. For the mass transfer between gas and liquid phases, the interfacial resistance is usually studied by the stagnant-film models, in which gas transfer to a quiescent liquid subphase with adsorbed or spreading surfactant film on top is monitored.[24−26] In these stagnant-film models, the effects of hydrodynamics are largely precluded by minimizing the system movement. Hence, it is possible to study the physicochemical effects exclusively. Using the stagnant-film models, previous studies found that monolayers of insoluble surfactants significantly retard gas transfer and this retardation is dependent not only on the surface pressure (i.e., closeness of packing of the film-forming molecules) but also on the chain length and headgroups.[24,25] On the other hand, soluble surfactants can increase gas transfer due to the increased interfacial movement caused by the Marangoni effect.[26]

The conventional experimental methodologies used to study the effect of surfactant on the interfacial gas transfer, however, have a number of limitations.

First, these methods are not capable of simultaneously measuring the surface tension and gas transfer. Therefore, the effect of dynamic surface tension, indicating the evolution of film structure and conformation,[29] on the gas transfer cannot be evaluated. In these methods, the surface tensions are usually measured separately by means of the Du Noüy ring method,[3,25] the drop weight method,[22] and the maximum bubble pressure method.[6] These methods (except for the maximum bubble pressure method) usually do not allow the measurement of dynamic surface tension.[30] And, more importantly, they do not allow the simultaneous measurements of surface tension and gas transfer. Theoretically, the combination of Langmuir trough and Wilhelmy balance does allow simultaneous measurements of surface tension and gas transfer.[31] However, the minimum surface tension that can be studied by that combination is limited due to the well-known problem of film leakage.[32]

Second, for these bubble methods, it is generally difficult to estimate the interfacial area. The bubbles are usually assumed to be spheres or simple axisymmetric bodies of revolution.[11] Deformation of the bubbles due to low surface tensions or movement is considered in indirect ways, such as the introduction of shape factor[20] or correction factor based on the eccentricity.[19] These approaches are neither accurate nor flexible.

Third, for these film methods, only highly soluble gases, such as hydrogen sulfide (H_2S),[24] sulfur dioxide (SO_2),[25] carbon dioxide (CO_2),[24,25] and ammonia,[26] can be studied. This limitation is due to the low sensitivity of these conventional methods. However, the use of these highly soluble gases causes a problem of convective instability:[25] due to their high solubility, dissolution of these gases can alter the local density of the subphase, thus inducing buoyancy-driven convection. This convective effect is not desired in the study of interfacial resistance, in which a static system is preferred, i.e., hydrodynamic effects should be excluded.

Therefore, the aims of this paper are to develop an experimental strategy capable of simultaneously measuring dynamic surface tension and interfacial gas transfer at air−water interfaces. Since the dynamic surface tension indicates the change in the film structure and conformation, it is possible to evaluate the effect of adsorbed surfactant film (i.e., interfacial resistance) on gas transfer.

2. Materials and Methods

2.1. Theoretical. *2.1.1. Steady-State Gas Transfer Model Based on ADSA-CB.* The methodology proposed is axisymmetric drop shape analysis in conjunction with a captive bubble (ADSA-CB). ADSA is a surface tension measurement methodology first introduced by Rotenberg et al.[33] As a drop-shape method, ADSA determines the surface tension by fitting an experimental drop/bubble profile to a family of theoretical profiles generated by numerical integration of the classical Laplace equation of capillarity. Surface tension of the drop/bubble is that of the best-matched Laplacian curve.

The CB arrangement was first introduced by Schürch et al.[34] In this strategy, the surface tension of a liquid sample is determined by monitoring the shape of a CB immersed in the liquid. The ceiling of the CB chamber is coated with hydrophilic materials, e.g., 1% agar gel, which ensures that the bubble is separated from the ceiling by a thin wetting film of the surrounding aqueous liquid, thus avoiding actual contact of the bubble with any solid support and eliminating all potential pathways for film leakage. The leakage-proof environment of a CB arrangement allows studies of ultralow surface tensions, such as those in lung surfactant systems.[34]

The combination of ADSA and a CB was first introduced by Prokop et al.[35] for the measurement of surface tensions of lung surfactant systems. Recently, a new version of ADSA-CB was developed.[36,37] Featuring an advanced image analysis scheme, this new version facilitates accurate measurements of surface tension and other information pertinent to the bubble geometry, such as area, volume, and curvature at the apex.[37] All the output of ADSA-CB can be readily used in the study of gas transfer from a static bubble to a quiescent liquid subphase. In the presence

(27) Goodridge, F.; Robb, I. D. *Ind. Eng. Chem. Fundam.* **1965**, *4*, 49.
(28) Nguyen Ly L. A.; Carbonell, R. G.; Mc-Coy, B. J. *AIChE J.* **1979**, *25*, 1015.
(29) Chang S.-H.; Franses E. I. *Colloids Surf., A* **1995**, *100*, 1.
(30) Adamson, A. W. *Physical Chemistry of Surfaces*, 5th ed.; John Wiley and Sons: New York, 1990.
(31) Cammenga, H. K.; Koenemann, D. *Thin Solid Films* **1988**, *159*, 53.
(32) Goerke, J.; Clements, J. A. In *Handbook of Physiology: The Respiratory System*; Macklem, P. T., Mead J., Eds.; American Physiology Society: Bethesda, MD, 1986; p 247.
(33) Rotenberg, Y.; Boruvka, L.; Neumann, A. W. *J. Colloid Interface Sci.* **1983**, *93*, 169.
(34) Schürch, S.; Bachofen, H.; Goerke, J.; Possmayer, F., *J. Appl. Physiol.* **1989**, *67*, 2389.
(35) Prokop, R. M.; Jyoti, A.; Eslamian, M.; Garg, A.; Mihaila, M.; del Río, O. I.; Susnar, S. S.; Policova, Z.; Neumann, A. W. *Colloids Surf., A* **1998**, *131*, 231.
(36) Zuo, Y. Y.; Ding, M.; Bateni, A.; Hoorfar, M.; Neumann, A. W. *Colloids Surf., A* **2004**, *250*, 233.
(37) Zuo, Y. Y.; Ding, M.; Li, D.; Neumann, A. W. *Biochim. Biophys. Acta* **2004**, *1675*, 12.

of a surfactant film adsorbed on the bubble surface, it is hence possible to evaluate the effect of interfacial resistance on the gas transfer.

The principle of this method is as follows. If one introduces a CB containing gas with a higher partial pressure than that in the liquid phase, gas transfer from the bubble to the liquid will occur according to

$$R = k_L A(C_A^* - C_A^0) \tag{1}$$

where, R is the average rate of gas transfer over the time of observation in mg/s; k_L is the mass transfer coefficient in cm/s; A is the mass transfer area in cm^2; and C_A^* and C_A^0 are the gas concentrations at the gas−liquid interface and in the bulk phase, respectively, in mg/cm^3. After formation of the bubble (i.e., time zero), C_A^* can be assumed to be constant and equal to the saturation concentration in equilibrium with the gas in the bubble. In other words, C_A^* can be correlated to the gas partial pressure in the bubble by Henry's law. C_A^0 is the average concentration of the dissolved gas in the bulk liquid, which is supposed to be unchanged throughout the observation. That is, the transferred gas from the bubble does not cause any appreciable concentration change in the body of the liquid. This assumption is valid if (1) the liquid phase is much larger than the gas phase or (2) the amount of gas transfer is small, i.e., both the time and area of contact should be limited. These two points can be guaranteed according to the experimental setup and protocol described later.

Equation 1 is a steady-state mass transfer equation, in which the compositions of the liquid and gas phases, averaged over a specific region and also with respect to any temporal fluctuations, are assumed to be statistically constant. The validity of eq 1 has been established in numerous experimental studies, provided that certain conditions are met.[38] The key ones are that the temperature and diffusivity at the surface should not be very different from those in the bulk of the liquid and that no chemical reaction occurs, so that all molecules of dissolved gas are in the same condition.[38]

Even though simple in format, eq 1 reveals the key factors influencing the interfacial gas transfer: driving force (i.e., the concentration gradient across the interface, $C_A^* - C_A^0$), interfacial area (A), and the physicochemical effects of the interface represented by k_L. Again, the k_L used in eq 1 is an average value. The instantaneous mass transfer coefficient may indeed vary from point to point and from time to time. However, for the purpose of studying and comparing the interfacial resistance of surfactant films, it is adequate and more reliable to use the average mass transfer coefficient since it is less affected by the random noise of the measurement. The average k_L can be evaluated as follows.

First, the average Laplace pressure (ΔP) in a CB should be calculated. The Laplace pressure at a given height of the CB (ΔP_h) (eq 2) is the sum of the Laplace pressure at the bubble apex and the local hydraulic pressure, which increases linearly along the entire height of the bubble (H_B), measured from the apex to the three-phase contact line.

$$\Delta P_h = \frac{2\gamma}{R_0} + \Delta\rho g h \tag{2}$$

In eq 2, the excess pressure at the bubble apex due to curvature is expressed using the Laplace equation for a spherical shape: γ is the surface tension; R_0 is the radius of curvature at the bubble apex; $\Delta\rho$ is the density difference across the interface; g is the local gravitational acceleration; and h is the vertical distance of any point of the bubble from the apex (see Figure 1). Therefore, the average Laplace pressure in a CB is

$$\Delta P = \frac{\int_0^{H_B} \Delta P_h \, dh}{H_B} = \frac{2\gamma}{R_0} + \frac{H_B}{2}\Delta\rho g \tag{3}$$

Second, the gas partial pressure (P^g) in a CB has to be evaluated. Even though a single-component gas is used to form a bubble, the bubble may consist of at least two components: the gas and the water vapor. The effect of water vapor is essentially to dilute the gas in a bubble. If the water vapor is in equilibrium with the aqueous solution, the vapor partial pressure (P^v) can be approximated to the saturation pressure of water at the experimental temperature. (See Supporting Information for a detailed thermodynamic derivation.) For example, at 37 °C, P^v is equal to 47.48 mmHg, which is approximately 6% of one atmospheric pressure. Therefore, according to Dalton's law, the effect of the water vapor can be removed by subtracting it from the total pressure of the bubble

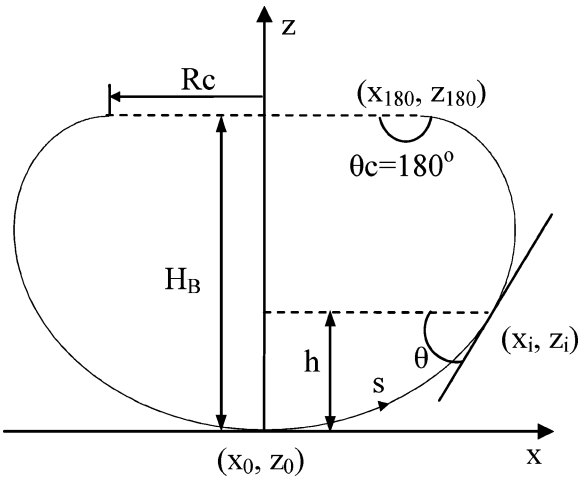

Figure 1. The meridian interface of the theoretical profile of a captive bubble.

$$P^g = P^l + \Delta P - P^v \tag{4}$$

where, P^l is the pressure in the liquid subphase.

It should be noted that cumulating evidence from our laboratory shows that a CB is not saturated with water vapor unless the gas is humidified before bubble formation [unpublished data]. The relative humidity in a CB has not been measured. However, in terms of gas partial pressure, the possible error due to undersaturation is less than 6% at 37 °C.

Third, by assuming the gas/vapor mixture in the bubble as an ideal gas, the mass of gas (M) can be calculated using the ideal gas law:

$$M = \frac{P^g V}{\bar{R}T} \tag{5}$$

where V is the volume of the bubble in cm^3, $\bar{R}$ is the ideal gas constant, 8.314 J/(mol K), and T is the experimental temperature in K.

Finally, k_L is expressed as

$$k_L = \frac{R}{A(C_A^* - C_A^0)} = \frac{1}{N}\sum_{i=1}^{N} \frac{\Delta M_i}{A_i \Delta t_i \left(\frac{P^g}{H} - C_A^0\right)} \tag{6}$$

where N is the number of discrete ADSA results (N is dependent on the rate of image acquisition), H is Henry's law constant in atm/(mg/cm^3), ΔM_i is the mass transfer within the time interval Δt_i. Equation 6 calculates the average k_L over the observation. It is also noted that the real-time gas transfer area (A_i) is used since the area varies with bubble shrinkage and surface tension variation in the presence of surfactant.

2.1.2. Determination of Bubble Geometry Using ADSA-CB. Key output of ADSA-CB is the surface tension, bubble area and volume, and curvature at the apex.[37] As mentioned before, ADSA determines surface tension and curvature at the apex by numerically fitting the experimental profile to the theoretical profiles based on the classical Laplace equation. After the best-

(38) Danckwerts, P. V. *Gas−liquid Reactions*; McGraw-Hill: New York, 1970.

matched theoretical profile is identified, the subsequent calculation of bubble area and volume is essentially independent from the experimental profile but performed using the best-matched theoretical one. This calculation is done by numerical integration of the theoretical profile to a user-specified boundary using eqs 7 and 8 (see Figure 1 for the meridian interface of a theoretical bubble profile and the corresponding coordinate system). The boundary value invoked in the case of a CB is a 180° contact angle. It is determined from the well-known assumption by Padday and Pitt,[39] who suggested that a sessile drop or captive bubble resting against a plane solid surface, but separated from the surface by a thin film of the surrounding fluid, possesses a contact angle of 180°. In a CB arrangement, this thin film is generated by complete wetting of the chamber ceiling by the surrounding aqueous liquid.

The surface area and volume of the bubble are given by

$$A_e = A_l + A_c = 2\pi \int_0^{s_{180}} x \, ds + \pi(x_{180} - x_0)^2 \quad (7)$$

$$V = \pi \int_0^{z_{180}} x^2 \, dz + \pi \int_0^{s_{180}} x^2 \sin\theta \, ds \quad (8)$$

In eq 7, the entire bubble area (A_e) consists of two parts: the lateral area (A_l) at the bubble−bulk liquid interface and the contact area (A_c) at the bubble−wetting film interface. As seen from Figure 1, A_l is Laplacian, but A_c is planar. Since the numerical integration stops at the contact angle of 180°, the contact radius (R_c) of this planar region can be easily calculated from the horizontal distance between the terminal point and the origin, i.e., $x_{180}-x_0$. Similarly, the height of the bubble (H_B) can be calculated from their vertical distance, $z_{180}-z_0$.

It should be noted that the gas transfer area used in eqs 1 and 6 is the lateral area (A_l) instead of the entire bubble area (A_e). This determination is due to the fact that the wetting film within the bubble−ceiling contact region is so thin (i.e., <500 nm[39]) that it will be soon saturated with gas, thus eliminating gas transfer from this part of the bubble. Detailed validation of this point can be found later in this paper.

2.2. Materials. The surfactant tested in this study is an exogenous lung surfactant preparation called Bovine Lipid Extract Surfactant (BLES; BLES Biochemicals, Inc., London, ON, Canada). It is prepared from bovine natural lung lavage. BLES contains approximately 98% phospholipids and 2% proteins by weight. The main tensioactive component in BLES is dipalmitoyl phosphatidylcholine (DPPC), accounting for approximately 45 wt%. BLES is stored frozen in sterilized vials with an initial concentration of 27 mg/mL. It is diluted to 0.5 mg/mL by a salt solution of 0.6% NaCl and 1.5 mM $CaCl_2$ on the day of the experiment. The water used in the experiments is demineralized and doubly distilled. The gas tested in this study is oxygen, with a minimum purity of 99.06% (BOC, Canada).

2.3. Experimental. The experimental setup is schematically shown in Figure 2. The CB chamber comprises three metal plates made of stainless steel and two viewing windows. Before each experiment, the chamber was assembled by sandwiching the two windows within the metal plates. The middle plate is essentially a spacer to provide the reservoir with a capacity of about 1 mL. The top of the reservoir is slightly concave, with a radius of 3 in. The concave surface serves as a "ceiling" to confine the bubble.

An oxygen bubble (~20 μL) was injected into the chamber by means of a microsyringe (50 μL, #1705, Gastight, Hamilton Corp, Reno, NV) through a side port of the chamber. During the injection, the tip of the needle was so close to the ceiling that the bubble immediately rested against the ceiling without traveling in the subphase. The interval of bubble injection was less than 5 s.

Image acquisition commenced immediately after the bubble formation and lasted for 5 min at a rate of up to 30 images per second. During image acquisition, the bubble was illuminated by a light source (Model V-WLP1000, Newport Corp, Fountain Valley, CA). A diffuser made of frosted glass was placed between the light source and the chamber to provide uniform incident light. The image acquisition system consists of a microscope (Apozoom, Leitz Wetzlar, Germany), a CCD camera (Model 4815-5000, Cohu Corp, Poway, CA), and a digital video processor (Parallax Graphics, Rocklin, CA). The microscope was equipped with a polarizing filter that reduced the glare and enhanced the contrast of the bubble image. The digital video processor performed both frame grabbing and image digitizing. Each image was digitized to a matrix of 640 × 480 pixels with 256 gray levels for each pixel, where 0 represents black and 255 represents white. The acquired images were stored in a SUN workstation (Sparc Station-10, Sun Microsystems, Inc., Santa Clara, CA) for further analysis by ADSA-CB. The entire setup except the computers was mounted on a vibration-free table (Technical Manufacturing Corp, Peabody, MA) to minimize the effects of external vibration.

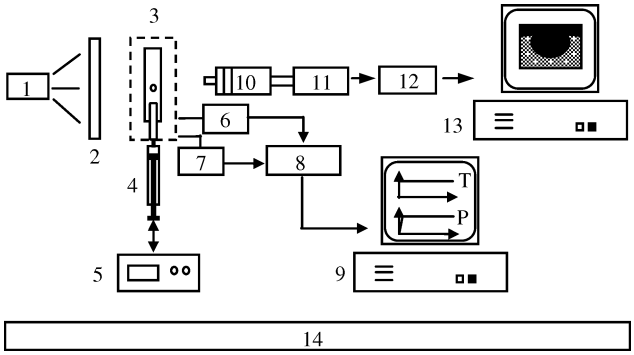

Figure 2. Schematic of the captive bubble setup: 1. light source; 2. diffuser; 3. thermostated captive bubble chamber; 4. motor-driven syringe; 5. motor controller; 6. thermocouple; 7. pressure transducer; 8. universal data acquisition card; 9. PC; 10. microscope; 11. CCD camera; 12. digital video processor; 13. workstation; and 14. vibration-free table.

The chamber temperature was thermostatically maintained at 37 ± 0.2 °C by a water bath (Model RTE-111, Neslab Instruments, Inc., Portsmouth, NH). An ultrafine thermocouple (AWG40, T type, Teflon insulated, Omega Eng. Inc, Laval, Quebec, Canada) was used to monitor the temperature in the chamber.

To examine the effect of a compressed film on gas transfer, the bubble (with adsorbed lung surfactant film) was compressed by adding liquid into the chamber by means of a motor-driven syringe (5 mL, #1005, Gastight, Hamilton Corp). The compression was completed within 2 s. Thereafter, the gauge pressure of the liquid subphase was maintained during the experiment and continuously monitored by a pressure transducer (DP15 with No. 40 diaphragm, Validyne Eng Corp, Northridge, CA). A universal data acquisition card (UPC601−U, Validyne) installed in a PC was used to simultaneously process both the pressure signal generated by the pressure transducer and the temperature signal generated by the thermocouple.

Different liquids were tested on different days. Approximately 15−20 runs were conducted for each liquid. For each run, a fresh oxygen bubble was injected into the chamber and released after 5 min. After each run, the liquid in the chamber was replaced to prevent local saturation. The results of mass transfer coefficients in different liquids were averaged from at least three satisfactory runs unless otherwise indicated. Criteria to discard certain experimental runs were based on the surface tension measurements. For instance, a water experiment was qualified only when (1) the mean value of the surface tensions deviated from the literature value[40] no more than 1 mJ/m^2 and (2) the standard deviation of the measurements was less than 1 mJ/m^2. For a lung surfactant sample, an experimental run was qualified only when (1) the initial surface tension at the onset of the recording was less than 30 mJ/m^2, indicating almost complete film formation during the interval of forming the bubble. This ensured that the subsequent gas transfer was studied under the influence of the adsorbed surfactant film, and (2) the surface tension decreased to the equilibrium values (i.e., 22−25 mJ/m^2) after 5 min of observation, indicating satisfactory surface activity.

(39) Padday, J. F.; Pitt, A. R. *Proc. R. Soc. London A.* **1972**, *329*, 421.

(40) Vargaftik, N. B.; Volkov, B. N.; Voljak., L. D. *J. Phys. Chem. Ref. Data* **1983**, *12*, 817.

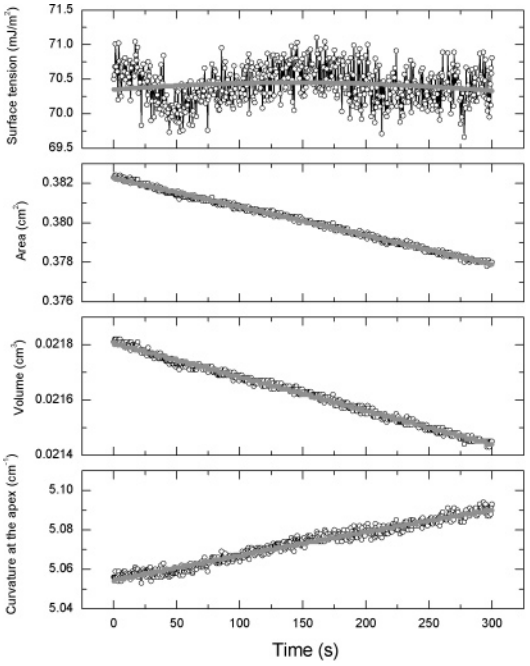

Figure 3. Output of ADSA-CB (surface tension, bubble area, volume, and curvature at the apex) for the gas transfer from an oxygen bubble to distilled water at 37 °C. Circular symbols, experimental results; light gray lines, smoothed results using SG filter.

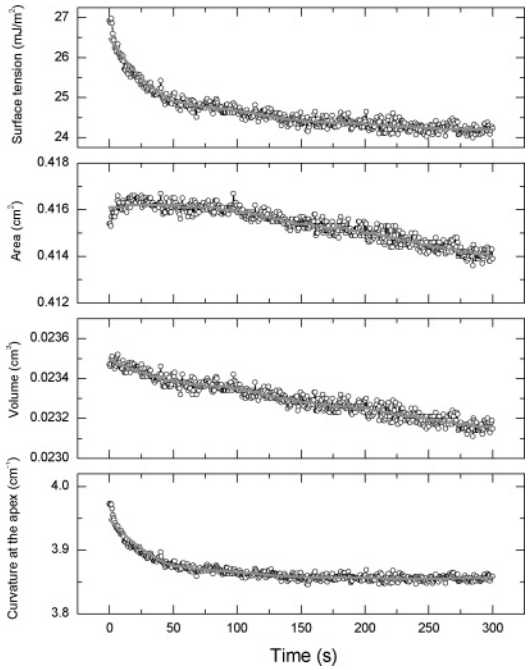

Figure 4. Output of ADSA-CB (surface tension, bubble area, volume, and curvature at the apex) for the gas transfer from an oxygen bubble to 0.5 mg/mL BLES at 37 °C. Circular symbols, experimental results; light gray lines, smoothed results using SG filter.

2.4. Data Processing. The results output by ADSA-CB showed slight local fluctuation, e.g., less than 0.5 mJ/m^2, in the surface tension. Before applying the ADSA results to the mass transfer model developed above, the Savitzky−Golay (SG) filter[41,42] was used to smooth the ADSA results.

3. Results

3.1. Effect of the Spontaneously Adsorbed Surfactant Film. Figures 3 and 4 show typical output of ADSA-CB (indicated by the circular symbols) for oxygen transfer in water and in 0.5 mg/mL BLES, respectively. Also in Figures 3 and 4 are the smoothed results (indicated by the light gray lines) using the SG filter. As shown in Figure 3, the surface tension of water is approximately constant over the observation, i.e., 70.4 ± 0.3 mJ/m^2. (The literature value is 70.05 mJ/m^2.[40]) The area and volume of the bubble linearly decrease, indicating gas transfer from the bubble to the liquid phase. The bubble curvature at the apex increases linearly, also suggesting bubble shrinkage. On the other hand, surface tension of BLES (see Figure 4) decreases from 26.9 to 24.2 mJ/m^2 after 300 s. Accompanied with the decrease in surface tension (especially in the initial 50 s) is a decrease in the bubble curvature, indicating the bubble flattening. The bubble volume decreases due to gas transfer. The bubble area is controlled by the simultaneous shape deformation due to surface tension decrease and size shrinkage due to gas transfer.

Surface tension and k_L measured from different experimental runs for water and for 0.5 mg/mL BLES are listed in Table 1 (see Supporting Information for reproducibility of the measurements). The surface tensions of water measured from individual runs are shown in the manner of mean ± standard deviation (SD). The SD indicates the scatter of the individual measurement. For BLES, the surface tensions at the onset and after 300 s are shown in Table 1. The surface tension and k_L evaluated from the different runs are shown in the manner of mean ± standard error of the mean (SEM). The SEM indicates the reproducibility of different experimental runs. It is noted that the ratio of the mass transfer coefficients of oxygen in BLES and in water is 0.82. It implies that the existence of adsorbed lung surfactant film near the equilibrium surface tensions shows a blocking effect on oxygen transfer from a CB.

3.2. Effect of the Compressed Surfactant Film. The effect of compressed surfactant film on oxygen transfer was examined by applying a pressure of 8 psi to the liquid subphase. This pressure causes approximately a 50% compression on the area of the adsorbed BLES film. Correspondingly, the surface tension decreases to 2.57 ± 0.08 mJ/m^2. The mass transfer coefficient calculated for this case is 1.95 × 10^{-4} cm/s, i.e., it is higher than that of the noncompressed films (i.e., 1.46 × 10^{-4} cm/s).

However, taking this result at face value would be misleading. As the pressure of the liquid subphase is increased by compression, the pressure in the CB is increased as well. This increase in the gas pressure may affect the liquid-phase mass transfer coefficient (k_L). The effect of pressure on k_L is still controversial.[43−45] Thus, k_L values measured at different pressures may not be directly comparable. To circumvent this problem, the effects of compressed surfactant films should be evaluated by comparison with the gas transfer in water (without a surfactant film) at the same controlled subphase pressure.

As a baseline, a controlled experiment was performed by applying and maintaining the same subphase pressure (i.e., 8 psi) in water. The measured k_L is 2.50 × 10^{-4} cm/s, i.e., it is also higher than that in water without compression (i.e., 1.77 × 10^{-4} cm/s). However, the ratio between the mass transfer coefficients of oxygen in BLES and in water

(41) Savitzky, A.; Golay, M. J. E. *Anal. Chem.* **1964**, *36*, 1627.
(42) Luo, J. W.; Ying, K.; He, P.; Bai, J. *Digital Signal Process.* **2005**, *15*, 122.
(43) Yoshida, F.; Arakawa, S. *AIChE J.* **1968**, *14*, 962.
(44) Dewes, I.; Kueksal, A.; Schumpe, A. *Chem. Eng. Res. Des.* **1995**, *73*, 697.
(45) Shin, S. K.; Kim, K. K.; Kim, K. *J. Ind. Eng. Chem.* **1995**, *1*, 6.

Table 1. Surface Tension (γ, mJ/m^2) and Mass Transfer Coefficients ($k_L \times 10^4$, cm/s) of an Oxygen Bubble in Water and in 0.5 mg/mL BLES at 37 °C

runs		a	b	c	d	e	mean ± SEM[c]
water	γ^a	69.9 ± 0.2	70.6 ± 0.3	70.4 ± 0.3	70.7 ± 0.2	70.7 ± 0.3	70.5 ± 0.2
	k_L	1.87	1.78	1.66	1.79	1.75	1.77 ± 0.03
BLES	γ^b	28.0−24.3	27.0−23.8	29.1−24.2	28.6−24.2	29.2−24.1	28.4 ± 0.4−24.1 ± 0.1
	k_L	1.36	1.53	1.44	1.41	1.55	1.46 ± 0.04

[a] Surface tensions of water are shown as mean ± standard deviation (SD). SD is calculated from the surface tensions measured over the 300 s of observation. [b] Surface tensions of BLES are shown as the initial value − the value after 300 s. [c] The final results are shown as mean ± standard error of the mean (SEM).

for this case of high compression is 0.78, which is 4% less than the case without compression, indicating an increased retardation of gas transfer.

Sosnowski et al. found that compressed DPPC films significantly impede oxygen transfer by up to 30%.[46] Therefore, the retardation found here is not surprising. However, this retardation is less than for a pure DPPC film and is presumably due to the presence of hydrophobic apoproteins (i.e., SP-B and SP-C), which are associated with the interface even at high surface pressures.[47]

4. Discussion

The present work is breaking new ground. It is therefore important to summarize the key assumptions made in establishing the gas transfer model: (1) the liquids in use are initially saturated with air; (2) the oxygen concentration in the liquid subphase remains unchanged during the experiment; (3) the solubility of oxygen, i.e., Henry's law constant, in a dilute lung surfactant sample (0.5 mg/mL) is the same as that in water; and (4) the mass transfer area does not include the part of the bubble in contact with the wetting film. These four assumptions are validated as follows.

4.1. DO before the Experiments. The initial concentration of dissolved oxygen (DO) was measured using an electrometric method, in which a DO probe (Mini Clark style electrode, #730, Diamond General, Ann Arbor, MI) in conjunction with a polarographic amplifier (Model 1900, A-M Systems, Sequim, WA) was used to measure the amount of DO. It was found that after exposure to atmosphere for at least 4 h, all tested liquids gave a reading of oxygen partial pressure of approximately 21%, which suggested that the liquids were saturated with air.

4.2. DO after the Experiments. The DO after each run was also measured. No detectable increase in the DO was found. This is due presumably to the short exposure time (i.e., 5 min) and the small gas transfer area of a single bubble (~0.4 cm^2). After 5 min, less than 2% of the bubble is dissolved (see Supporting Information), accounting for about 0.5 μg. It is 10 times smaller compared with the initial amount of the DO in the subphase, i.e., 6.84 μg of O_2 in 1 mL of aqueous liquid at 37 °C and at atmospheric pressure.

Oxygen transfer was also studied for an extended time period, i.e., 30 min. It was found that after 30 min, approximately 2 μg of O_2 was dissolved in the liquid subphase, i.e., approximately 30% of the initial amount of DO. Therefore, under these circumstances, the assumption of constant oxygen concentration in the subphase is violated due to the accumulation of DO.

In addition to the short exposure time, replacing the liquid subphase after every experimental run also helps maintain a constant DO level. It should also be noted that instantaneous local increase in the oxygen concentration due to the dissolution of the bubble may occur. However, the use of the steady-state mass transfer model tends to average out this effect.

4.3. Oxygen Solubility in a Dilute BLES Sample. Oxygen solubility in 0.5 mg/mL BLES was also measured. It was found to be the same as that in water. However, there may be an artifact since the DO probe can only detect the free oxygen molecules which are able to move across the membrane. If oxygen molecules bind with the phospholipid or protein molecules in BLES, the solubility measured by the DO probe could be less than the actual value. Oxygen solubility in aqueous dispersions of phospholipid bilayers may be indeed different from that in water. Using a modified Winkler method, Smotkin et al.[48] found that oxygen solubility in a 1.5% w/w dimyristoyl phosphatidylcholin (DMPC) aqueous dispersion was critically dependent on the gel-to-liquid crystal phase transition temperature (T_c) of the lipid. When the temperature was below T_c, i.e., 24 °C for DMPC, the oxygen solubility in DMPC aqueous dispersion was approximately the same as that in water at the same temperature; at a temperature above 24 °C, however, oxygen was found to be 3−4 times more soluble in the lipid dispersion. If this finding can be generalized to other phospholipids, such as DPPC (DPPC is the main phospholipid component in BLES, accounting for 45 wt%.), the oxygen solubility in a dilute DPPC aqueous suspension (~1.5% w/w) at 37 °C should be similar to that in water since DPPC has a T_c of approximately 41 °C. Moreover, the phospholipid concentration currently in use, i.e., 0.5 mg/mL or 0.05% w/w, is 30 times more dilute than that tested by Smotkin et al..[48] Therefore, it is not likely that the oxygen solubility in 0.5 mg/mL BLES sample significantly deviates from that in water.

4.4. Gas Transfer in the Wetting Film. The wetting film between a CB and the ceiling of the chamber is not visible since it is shielded by the concave ceiling. Therefore, it is not possible to conduct direct measurement of its thickness. However, thickness of the wetting film can be approximated indirectly using the available disjoining pressure data. By means of an interferometric technique, Read and Kitchener[49] measured the thickness of a flat wetting film of electrolyte solutions. They found that, at a disjoining pressure of 145 Pa, the thickness of a wetting film is in the order of 100 nm.[49] The disjoining pressure of a wetting film generated by a CB is equal to the Laplace pressure inside the bubble.[50] The Laplace pressure of typical CBs ranges from 30 to 90 Pa, depending on the surface tension (see Supporting Information for a plot of Laplace pressures of CBs). Since the thickness of a wetting film increases with a decreasing disjoining pressure, the

(46) Sosnowski, T. R.; Gradoñ, L.; Skoczek, M.; Drozdiel, H. *Int. J. Occup. Saf. Ergon.* **1998**, *4*, 391.
(47) Putz, G.; Walch, M.; Van, E. M.; Haagsman, H. P. *Biochim. Biophys. Acta* **1999**, *1453*, 126.
(48) Smotkin, E. S.; Moy, F. T.; Plachy, W. Z. *Biochim. Biophys. Acta* **1991**, *1061*, 33.
(49) Read, A. D.; Kitchener, J. A. *J. Colloid Interface Sci.* **1969**, *30*, 391.
(50) Derjaguin, B. V.; Churaev, N. V.; Muller, V. M. In *Surface Forces*; Kitchener J. A., Ed.; Consultants Bureau: New York, 1987; p 327.

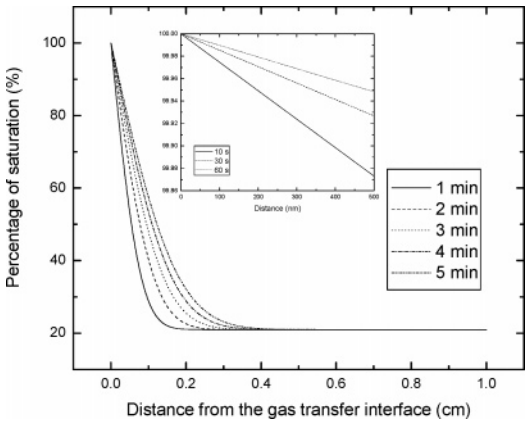

Figure 5. Theoretical profiles of gas concentration calculated from 1D diffusion equation. Inset: the profiles of gas concentration in the region of wetting film (i.e. <500 nm) after contact with a CB for 10, 30, and 60 s.

wetting film in a CB arrangement should be no less than 100 nm in thickness. Padday and Pitt[39] suggested that the wetting film is no more than 500 nm thick. Therefore, we draw the conclusion that the thickness of the wetting film in a CB arrangement is in the range of 100−500 nm.

Gas concentration in the wetting film can be approximated by solving the one-dimensional unsteady-state diffusion equation (see Supporting Information for a detailed derivation). Figure 5 shows the calculated curves of gas concentration (in the format of percentage of saturation) as a function of distance from the gas transfer interface (i.e., the bubble surface) after different intervals of exposure. As seen in Figure 5, oxygen transport in the time period of 5 min extends only over approximately 4 mm. The inset in Figure 5 shows that, at a distance from the air−liquid interface of 500 nm, the oxygen concentration is 99.86% of the saturation concentration after only 10 s. This result implies that the liquid film at the ceiling of the chamber is essentially saturated with oxygen by the time data acquisition starts. Therefore, it is reasonable to assume that no actual gas transfer occurs at this part of the bubble.

Correct evaluation of the gas transfer area is vital to the estimation of the mass transfer coefficient. For a CB in water, the area in contact with the wetting film at the ceiling (A_c) accounts for less than 6% of the entire bubble area; in contrast, for a lung surfactant system at equilibrium surface tensions, the contact area accounts for approximately 12%. For a compressed CB in lung surfactant, the contact area accounts for up to 25% due the low surface tension. Under this circumstance, using the entire bubble area as the gas transfer area would lead to inaccuracies.

5. Conclusions

By precisely monitoring the geometry of a single drop/bubble, ADSA shows potential for the study of transport phenomena involving an interface. In conjunction with a sessile drop, ADSA has been used to study the water permeability of polymer surfaces before.[51] In the present study, by monitoring the dissolution of a single static captive bubble in a quiescent liquid, ADSA demonstrates the feasibility to evaluate the effect of surfactant on interfacial gas transfer. ADSA-CB outperforms the conventional methods in a number of aspects. First, ADSD-CB is able to measure dynamic surface tension and interfacial gas transfer simultaneously, thus allowing the study of the effect of film evolution on the gas transfer. Second, ADSA-CB is capable of yielding detailed information pertinent to the geometry of a CB, such as its lateral and contact areas. Hence, it is possible to evaluate the effect of bubble shrinkage on gas transfer. Third, ADSA-CB allows for the study of very low surface tension (i.e., <5 mJ/m^2), which renders it applicable to lung-surfactant-related studies. Fourth, ADSA-CB does not require equilibrium in gas transfer. Consequently, reproducible experiments can be conducted within a short time interval.

ADSA-CB was used here to study the effect of lung surfactant on oxygen transfer. For a spontaneously adsorbed film (i.e., near the equilibrium spreading surface tension, 22−25 mJ/m^2), k_L in BLES is 18% less than in water. At very low surface tensions ($\sim$2 mJ/m^2) caused by film compression, the lung surfactant film shows more retardation, i.e., a reduction of k_L by 22%. Compared with an earlier study of pure DPPC films,[46] this finding suggests that the lung surfactant films exhibit less blocking of oxygen transfer than pure DPPC films.

A limitation of the present method, compared with a stagnant-film method, is that the film compression and the bubble pressure are correlated. In other words, to compress the film adsorbed on a bubble, one has to increase the pressure in the liquid subphase, as well as in the bubble. This change in system pressure may cause the calculated mass transfer coefficients to be not directly comparable. This problem can be circumvented by comparing gas transfer in water (without a surfactant film) at the same controlled subphase pressure. Another limitation of this method is that only adsorbed surfactant film can be readily studied. Comparing to a film method, such as in a Langmuir trough, film-spreading in a CB arrangement is technically complicated, if not impossible.[52] Therefore, even though applicable in principle, ADSA-CB is more effective in the study of an adsorbed film than a spreading film. Nevertheless, the drop configuration and film formation due to adsorption are preferable to a film model in the study of lung surfactant due to its similarity to the in vivo conditions.

Acknowledgment. This work was supported by a grant from Canadian Institutes of Health Research (MOP-38037) and an Open Fellowship from University of Toronto to Y.Y.Z.. We also thank Dr. David Bjarneson of BLES Biochemicals, Inc. for his generous donation of the BLES samples.

Supporting Information Available: A detailed thermodynamic derivation of determining the equilibrium vapor pressure in a captive bubble (see Section 2.1.1.); reproducibility of the ADSA-CB in measuring oxygen transfer (see Sections 3.1 and 4.2); Laplace pressures of CBs (see Section 4.4); and A 1D unsteady-state diffusion equation and its solutions (See Section 4.4.). This material is available free of charge via the Internet at http://pubs.acs.org.

LA050281U

(51) Long, J.; Chen, P. *Langmuir* **2001**, *17*, 2965.

(52) Putz, G.; Walch, M. *Biophys. J.* **1998**, *75*, 2229.